Rydberg Radicals. 1. Frozen-Core Model for Rydberg Levels of the Ammonium Radical

S. Havriliak and Harry F. King*

Contribution from the Department of Chemistry, State University of New York at Buffalo, Buffalo, New York 14214. *Received April 2, 1982*

Abstract: Rydberg radicals are transient polyatomic species stable with respect to dissociation in excited electronic states but dissociative on the ground-state surface. This paper proposes that these systems be treated theoretically by Rayleigh–Schrödinger perturbation theory (RSPT) that reduces to a frozen-core model in zeroth order. Special computational techniques permit the use of very large Gaussian basis sets for the Rydberg orbital space. The zeroth-order equations are solved to high accuracy, probably to within 10 cm^{-1}, for Rydberg orbital energies of NH_4 as well as for the isoelectronic sodium atom. Energies, force constants, Coriolis coupling constants, Jahn–Teller parameters, orbital radii, and transition moments are reported for Rydberg states of the ammonium radical up through the $^2A_1(5s)$ level. Serious conflicts arise in comparing theoretical, spectroscopic, and molecular-beam results for NH_4 and ND_4. Some key areas for further investigation are outlined, e.g., resolution of the conflict between spectroscopic and molecular-beam values for the lifetime of the metastable ground state, and a 3000-cm^{-1} discrepancy between experimental and best theoretical estimate of the frequency of the Schuster band.

I. Introduction

Bernstein[1] was one of the first to suggest that free radicals of the type AH might be stable with respect to dissociation into A plus a hydrogen atom, where A is a closed-shell molecule with sufficiently large proton affinity such as NH_3 or H_2O. There exists in the literature conflicting experimental[2,3] and theoretical[2-6] evidence concerning such radicals. Very recently new experimental results bearing on this subject have begun to appear from two different sources, namely, high-resolution electronic spectroscopy[7-10] and neutralized-ion-beam experiments.[11] Motivated by these developments we have undertaken a series of accurate ab initio electronic-structure calculations of AH radicals. Herzberg's observation in 1979 of band spectra of triatomic hydrogen prompted theoretical studies of that system using a simple frozen-core model (Koopmans theorem).[12-14] The present paper extends that analysis to the NH_4 radical and defines a scheme, based on Rayleigh–Schrödinger perturbation theory, for systematically improving the theoretical model. As in the earlier study of triatomic hydrogen,[12] we report in this paper a number of spectroscopic properties obtained by using the frozen-core model, i.e., zeroth-order results in perturbation theory for low-lying excited states of NH_4. To estimate energy errors inherent in the frozen-core model we carry out a similar calculation for the isoelectronic sodium atom for which experimental results are readily available. The second paper in this series will be concerned with the dissociation process $NH_4 \rightarrow NH_3 + H$ on the ground-state potential energy surface, and so addresses issues more relevant to the beam experiments.[11] Subsequent papers deal with corrections coming from higher-order terms in the perturbation expansion.

The five lowest excited electronic states of H_3 and D_3 have now been well characterized by detailed analyses of four electronic bands observed in emission.[8,9] Transitions to the dissociative ground state are too diffuse to be observed. Spectral lines involving transitions to the first Rydberg state (the lowest $^2A_1'$ state) are broadened corresponding to a lifetime of about 10^{-12} s[8] for that state. The higher Rydberg states have appreciably longer half-lives. All of these Rydberg states (the $^2A_1'$ state and higher electronic states) are stable with respect to dissociation into H_2 plus H, and all have very nearly the same geometry as that of the H_3^+ ion. Thus, one can think of the triatomic hydrogen radical as a gas-phase H_3^+ ion which has captured an electron in an outer orbital. The electron makes radiative transitions to lower and lower Rydberg levels until it finally decays into the ground electronic state at which point the molecule dissociates. Dabrowski and Herzberg have given the name "Rydberg radicals" to these transient polyatomic species which are stable only in excited states.[8]

Similar spectral information is becoming available for the ammonium radical[10] but is presently not nearly so complete as that for the prototype Rydberg radical H_3. Two band systems are currently under investigation, namely, the Schuster band observed near 5639 Å (near 5782 Å in ND_4) and the Schüler bands observed near 6635 Å (near 6750 Å in ND_4). Although some of these spectral features have been observed for over 100 years, only within the past year has it been established that the carrier is, in fact, the ammonium radical.[10]

A number of early theoretical investigations using the one-center expansion method treated the ammonium radical,[2,4,5] but only one of these[5] attempted to compute the Rydberg levels now thought to be responsible for the observed spectra. The present paper extends the early work of Strehl et al.[5] using a nearly complete, multicenter Gaussian orbital basis. Broclawik, Mrozek, and Smith have recently carried out electronic-structure calculations for the ammonium radical using the X-α method,[15a] and Raynor and Herschback (RH) have studied a series of first-row AH radicals using SCF methods in a Slater basis.[15b] A brief comparison of the Raynor–Herschback results with our more accurate NH_4 calculations is presented below.

Lathan et al. (LHCP) also used a multicenter Gaussian basis in a calculations of the ground-state potential energy surface for the ammonium radical.[6] They found no barrier for dissociation into ammonia plus a hydrogen atom. We return to this issue in paper 2 but merely comment here that instability predicted by LHCP is a spurious result due to orbital basis set deficiencies. Experimental evidence from fragmentation in radical beams im-

(1) H. J. Bernstein, *J. Am. Chem. Soc.*, **85**, 484 (1963).
(2) C. E. Melton and H. W. Joy, *J. Chem. Phys.*, **46**, 4275 (1967); *48*, 5286 (1968).
(3) K. S. E. Niblaeus, B. O. Roos, and E. M. Siegbahn, *Chem. Phys.*, **25**, 207 (1977), and references cited therein concerning the H_3O radical.
(4) J. I. Horvath, *J. Chem. Phys.*, **19**, 978 (1951); D. M. Bishop, *ibid.*, **40**, 432 (1964).
(5) W. Strehl, H. Hartmann, K. Hensen, and W. Sarholz, *Theor. Chim. Acta*, **18**, 290 (1970).
(6) W. A. Lathan, W. J. Hehre, L. A. Curtis, and J. A. Pople, *J. Am. Chem. Soc.*, **93**, 6377 (1971).
(7) G. Herzberg, *J. Chem. Phys.*, **70**, 4806 (1979).
(8) I. Dabrowski and G. Herzberg, *Can. J. Phys.*, **58**, 1238 (1980).
(9) G. Herzberg and J. K. G. Watson, *Can. J. Phys.*, **58**, 1250 (1980); G. Herzberg, H. Lew, J. J. Sloan, and J. K. G. Watson, *ibid.*, **59**, 428 (1981).
(10) G. Herzberg, *Faraday Discuss. Chem. Soc.*, **71**, 165 (1981).
(11) B. W. Williams and R. F. Porter, *J. Chem. Phys.*, **73**, 5598 (1980).
(12) H. F. King and K. Morokuma, *J. Chem. Phys.*, **71**, 3213 (1979).
(13) M. Jungen, *J. Chem. Phys.*, **71**, 3540 (1979).
(14) R. L. Martin, *J. Chem. Phys.*, **71**, 3541 (1979).
(15) (a) E. Broclawik, J. Mrozek, and V. H. Smith, Jr., in press; (b) S. Raynor and D. R. Herschbach, *J. Phys. Chem.*, submitted.

0002-7863/83/1505-0004$01.50/0

plies that ND_4 is metastable with a half-life of about 1 μs and an exothermicity of 0.22 eV. Our ab initio results are in qualitative agreement with this picture.

II. Computational Method

Perturbation Theory. Let the nonrelativistic electronic Hamiltonian for a Rydberg radical be expressed as

$$H = H^0 + H^1 \tag{1}$$

where

$$H^0 \equiv \sum_{i=1}^{NE} \mathbf{f}(i) \tag{2}$$

and **f** is the closed-shell Fock operator for the parent cation

$$\mathbf{f}(i) = -1/2\nabla_i^2 - \sum_{\alpha=1}^{NN} Z_\alpha r_{\alpha i}^{-1} + \sum_{l=1}^{NFCO} [2\mathbf{J}_l(i) - \mathbf{K}_l(i)] \tag{3}$$

The perturbation operator is

$$H^1 \equiv \sum_{i<j}^{NE} r_{ij}^{-1} - \sum_{i=1}^{NE}\sum_{l=1}^{NFCO} [2\mathbf{J}_l(i) - \mathbf{K}_l(i)] \tag{4}$$

The limiting summation indices NE, NN, and NFCO define the number of electrons, nuclei, and frozen-core orbitals, respectively.

From Rayleigh–Schrödinger perturbation theory (RSPT) the zeroth- and first-order equations are

$$(H^0 - E_k^0)\Psi_k^0 = 0 \tag{5}$$

$$(H^0 - E_k^0)\Psi_k^1 + (H^1 - E_k^1)\Psi_k^0 = 0 \tag{6}$$

The zeroth-order function is a Slater determinant of NFCO doubly occupied frozen-core orbitals plus a singly occupied virtual orbital of the parent cation.

$$\Psi_k^0 = A[\phi^c_1\bar{\phi}^c_1 \cdots \phi^c_{NFCO}\bar{\phi}^c_{NFCO}\phi_k] \tag{7}$$

$$\mathbf{f}\phi_k = \epsilon_k\phi_k \tag{8}$$

$$E_k^0 = 2\sum_{i=1}^{NFCO} \epsilon_i + \epsilon_k \tag{9}$$

The frozen-core energy, E_k^{FC}, is the expectation value of the true Hamiltonian averaged over the zeroth-order wave function. This is also the (RSPT) energy computed to first-order.

$$E_k^{FC} \equiv \langle \Psi_k^0 | \mathbf{H} | \Psi_k^0 \rangle = E_k^0 + E_k^1 = E_{core} + \epsilon_k \tag{10}$$

Here E_{core} is the SCF energy of the parent cation. Similarly, other properties, such as angular momentum, will be computed as the expectation value of the appropriate operator averaged over Ψ_k^0.

The first-order wave function, Ψ_k^1, consists of single excitations out of core orbitals (static core polarization) plus double excitations out of all occupied pairs. A consequence of our choice of H^0 is that single excitations out of the occupied Rydberg orbital, $\phi_k \rightarrow \phi_{k'}$, make no contribution to Ψ_k^1. In effect, the Rydberg orbital is optimized in the field of the core electrons, but the core is not optimized in the field of the Rydberg electron. This partial Brillouin theorem is an essential feature of a meaningful perturbation expansion because otherwise there would exist excitations with small energy denominators, e.g., $|\epsilon_{k'} - \epsilon_k| < 0.1$ eV. As it is, no contributions to Ψ_k^1 have energy denominators appreciably smaller than the HOMO–LUMO gap, which for NH_4^+ is 23.4 eV. The total contribution to the second-order energy correction, E_k^2, from all double excitations out of pairs of core orbitals is sizable. Although this can be important for, e.g., computation of proton affinity, it is of no importance for Rydberg spectroscopy since such double excitations make the same contribution to all Rydberg states. On the other hand, the smaller contribution from double excitations out of core–Rydberg pairs (dynamic core polarization) can be expected to perturb Rydberg spacings and so constitutes one of the important corrections not included in the calculations reported in this paper. In spite of these deficiencies in the frozen-core model, we solve the zeroth-order equations to high accuracy because they provide the foundation for the calculation of higher-order perturbation corrections to be reported in paper 3 of this series.

Computation of Virtual Orbitals. The traditional Roothaan closed-shell SCF procedure[16] is modified to permit use of two different orbital basis sets. The first set $\{\chi_\sigma^c | \sigma = 1, 2, ..., n_c\}$ defines the core space. Another larger set contains many diffuse functions in addition to functions in the core region. This we refer to as the Rydberg basis $\{\chi_\sigma | \sigma = 1, 2, ..., n\}$. The core basis, not necessarily a subset of the Rydberg basis, is used with the usual SCF iterative procedure to generate core orbitals, ϕ^c_i, and the Fock operator **f** for the ammonium ion. The computer program then retains these SCF results, reads in the Rydberg basis, and forms matrices **F**, **S**, and **B** with elements

$$F_{\sigma\rho} = \langle \chi_\sigma | \mathbf{f} | \chi_\rho \rangle \tag{11}$$

$$S_{\sigma\rho} = \langle \chi_\sigma | \chi_\rho \rangle \tag{12}$$

$$B_{\sigma i} = \langle \chi_\sigma | \phi^c_i \rangle \tag{13}$$

An orthonormal Rydberg basis is then defined by the transformation matrix **Q** which satisfies

$$\mathbf{Q}^\dagger\mathbf{S}\mathbf{Q} = \mathbf{I} \tag{14}$$

$$\mathbf{Q}^\dagger\mathbf{B} = \mathbf{O} \tag{15}$$

An algorithm for constructing a suitable **Q** matrix is given in the Appendix. Virtual orbital energies are obtained by diagonalizing the transformed Fock matrix.

$$(\mathbf{Q}^\dagger\mathbf{F}\mathbf{Q})\mathbf{V} = \mathbf{V}\epsilon \tag{16}$$

where **V** is unitary. The coefficient matrix for the virtual molecular orbitals is given by

$$\mathbf{C} = \mathbf{Q}\mathbf{V} \tag{17}$$

where

$$\phi_k = \sum_{\sigma=1}^{n} \chi_\sigma C_{\sigma k} \tag{18}$$

Note that eq 15, 17, and 18 assure that ϕ_k is rigorously orthogonal to all core orbitals. One could, alternatively, eliminate eq 15 and simply discard the five lowest eigenvalues and their vectors obtained in eq 16. The two methods are equivalent in the limit of complete basis sets; otherwise, our method provides an improved, i.e., lower, upper bound on the lowest virtual level of each symmetry.

The computer program is a modification of the HONDO SCF code.[17] All two-electron integrals $(\chi_\sigma\chi_\rho||\chi_\mu^c\chi_\nu^c)$ and $(\chi_\sigma\chi_\mu^c||\chi_\rho\chi_\nu^c)$ are accurately evaluated and used without being stored on an integral file. As each integral is generated, it is multiplied by the appropriate density matrix element and added into $F_{\sigma\rho}$. Point group symmetry is used to reduce the number of integrals computed.[18] Special subroutines are employed for very fast computation of single-center integrals. These techniques permit use of very large Rydberg bases which would otherwise be prohibitively expensive.

Basis Sets. Our χ_σ are contracted Cartesian Gaussian basis functions.

$$\chi_\sigma = x^{mx}y^{my}z^{mz}\sum_i b_i \exp(-a_i r^2)$$

We denote a set of primitives by round bracket notation, (/), and a set of contracted functions by square brackets, [/]. Functions to the left of the solidus are located on nitrogen, and those to the right on hydrogen. A d shell or f shell contains 6 or 10 functions, respectively. Our standard core basis is an (11s,7p,2d/5s,2p) set contracted to [6s,1p,1d/3s,2p] giving $n_c = 51$. This is a Dunning (10s,6p) set[19] augmented with a double set of polarization functions

(16) C. C. J. Roothaan, *Rev. Mod. Phys.*, **23**, 69 (1951).
(17) M. Dupuis, J. Rys, and H. F. King, *QCPE*, **12**, 336 (1977); *J. Chem. Phys.*, **65**, 111 (1976).
(18) M. Dupuis and H. F. King, *Int. J. Quantum Chem.*, **11**, 613 (1977).

Table I. Standard 51-Term Gaussian Core Basis Set (11s,7p,2d/5s,2p) Contracted to [6s,1p,1d/3s,2p][a]

	nitrogen-centered functions						hydrogen-centered functions			
	s-type		p-type		d-type		s-type		p-type	
	a_i	b_i	a_i	b_i	a_i	b_i	a_i	b_i	a_i	b_i
1	13520	0.000 760	35.91	0.005 383	1.3600	0.013 765	33.640	0.025 374	1.6500	1.0
2	1999	0.006 076	8.480	0.032 642	0.4000	0.019 658	5.0580	0.189 684	0.5500	1.0
3	440	0.032 847	2.706	0.103 579			1.1470	0.852 933		
4	120.9	0.132 396	0.9921	0.209 917			0.3311	1.0		
5	38.47	0.393 261	0.3727	0.253 004			0.1013	1.0		
6	13.46	0.546 339	0.1346	0.088 131						
7	13.46	0.252 036	0.0486	−0.005 773						
8	4.993	0.779 385								
9	1.569	1.0								
10	0.5800	1.0								
11	0.1923	1.0								
12	0.0222	1.0								

[a] Nitrogen p and d contraction coefficients are those for T_d symmetry with R_{NH} = 1.0098 Å.

Table II. Standard 149-Term Gaussian Rydberg Basis Set (20s,13p,11d/5s,1p) Contracted to [20s,13p,11d/3s,1p]

	nitrogen-centered functions						hydrogen-centered functions			
	s-type		p-type		d-type		s-type		p-type	
	a_i	n^a	a_i	n^a	a_i	n^a	a_i	c_i	a_i	c_i
1	18570	1	69.13	2	3.115	3	33.64	0.025 374	1.2000	1.0
2	6632	1	28.80	2	1.298	3	5.058	0.189 684		
3	2369	1	12.00	2	0.5408	3	1.147	0.852 933		
4	846.0	1	5.001	2	0.2253	3	0.3311	1.0		
5	302.1	1	2.084	2	0.0939	3	0.1013	1.0		
6	107.9	1	0.8681	2	0.0391	3				
7	38.54	1	0.3617	2	0.0163	3				
8	13.76	1	0.1507	2	0.0064	4				
9	4.915	1	0.0628	2	0.0032	4				
10	1.756	1	0.0340	3	0.0016	5				
11	0.6400	2	0.0170	3	0.0008	5				
12	0.3200	2	0.0085	4						
13	0.1600	2	0.0043	4						
14	0.0800	2								
15	0.0400	3								
16	0.0200	3								
17	0.0100	4								
18	0.0050	4								
19	0.0025	5								
20	0.0013	5								

[a] Principal quantum number.

on nitrogen and hydrogen plus an extra diffuse s and p shell on nitrogen to improve the tails of the core orbitals. Exponential parameters, a_i, and contraction coefficients, b_i, are given in Table I. Under T_d symmetry the 7p shells can be completely contracted without error. The two d shells have been assigned contraction coefficients corresponding to their values in the t(2p) orbital. This reduces the size of the density matrix which defines the Fock operator, and raises the computed value of E_{core} by only 36 μhartree. The p- and d-type contraction coefficients reported in Table I are optimized for NH_4^+ in T_d symmetry with R_{NH} = 1.0098 Å. They are reoptimized for each new value of R_{NH}; and for less symmetric geometries the p and d contraction scheme is relaxed accordingly. For example, an unsegmented [3p,2d] contraction is used when NH_4^+ is distorted to C_{3v} symmetry. In these cases, the p,d contraction error for E_{core} is a small fraction of 1 μhartree.

Our standard Rydberg basis is the 149-term [20s,13p,11d/3s,1p] set described in Table II. The nitrogen basis is uncontracted. The hydrogen s set is the same as that in the core basis. The nitrogen (20s) set consists of 10 even-tempered functions[20] with an exponent ratio of 2.8, plus 10 more diffuse functions with ratio 2.0. These parameters were varied to minimize the lowest Rydberg a-type orbital energy, probably to within a few microhartrees of its limiting value. Note that exponent ratios decrease with increasing quantum number as found by Jungen.[21] The third column of Table II indicates that two primitives describe the outer radial peak of the 4s function and two others describe the 5s radial peak. This assignment is based on the relative signs of the $C_{\sigma k}$ coefficients. It is also consistent with the computed radii of the Rydberg orbitals and the a_i values of the individual primitives. Note that the exponential parameter in an l-type primitive is related to its root mean square (rms) radius according to

$$\langle r^2 \rangle^{1/2} = [(2l + 3)/(4a_i)]^{1/2}$$

The (13p) set consists of nine even-tempered functions with an exponent ratio of 2.4, plus four more with ratio 2.0. These parameters were varied to minimize the lowest t_2-type Rydberg

(19) T. H. Dunning, Jr., *J. Chem. Phys.*, **55**, 716 (1971).

(20) R. C. Raffenetti, *J. Chem. Phys.*, **58**, 4452 (1973); M. W. Schmidt and K. Ruedenberg, *ibid.*, **71**, 3951 (1979).

(21) M. Jungen, *J. Chem. Phys.*, **74**, 750 (1981).

Table III. Comparison of Frozen-Core and Experimental Ionization Energies (in cm^{-1}) for the Sodium Atom in Rydberg States with Quantum Numbers n and l

	l =				
n	0	1	2	3	4
		Frozen-Core Model[a]			
3	39 893.9	24 015.5	12 217.2		
4	15 385.8	11 043.1	6 872.8	6858.6	
5	8 128.8	6 349.3	4 397.7	4389.9	4389.5
6	5 018.6	4 122.0	3 051.9	3048.2	3048.2
		Experiment[b]			
3	41 449.7	24 482.0	12 276.8		
4	15 709.8	11 179.1	6 900.9	6861.0	
5	8 249.0	6 407.7	4 412.9	4392.0	4389.5
6	5 077.0	4 152.3	3 062.4	3049.6	3048.2[c]
		Experiment − Theory			
3	1 555.8	466.5	59.6		
4	324.0	136.0	28.1	2.4	
5	120.2	58.4	15.2	2.1	0.0
6	58.4	30.3	10.5	1.4	0.0

[a] Negative virtual orbital energy of sodium ion, $-\epsilon$. 1 hartree = 219475 cm^{-1}. [b] From ref 22 averaged over spin-orbit multiplets. [c] This number does not exist in Moore's tables and was estimated by using the Rydberg formula.

orbital energy. The d-type basis was similarly constructed. The s-type subspace of the (11d) set strongly overlaps the space of the (20s) set. As a result, three linear combinations of nearly redundant functions are discarded as described in the Appendix. Tests indicate that truncation errors for this basis set are not greater than 10 μhartree for any orbital energy up through the 5s level. To achieve this precision it is necessary, even for Rydberg orbitals, to accurately describe the inner radial peaks using many Gaussians with large a_i values as indicated in Table II. Just two primitives per principal quantum number appear to be adequate for outer radial peaks.

For certain test calculations discussed below, we employ a third basis set with the description [20s,1p,1d,5f/3s,2p]. This set of 121 functions is obtained from the standard core basis by substituting the nitrogen (20s) set for the usual [7s] set and by adding five shells of f-type functions on nitrogen with the following exponents: (1.8, 0.4, 0.1, 0.03, and 0.01). This very nearly saturates both the core space and the a-type Rydberg space under T_d symmetry.

III. Results

Sodium Atom. It is of interest first to compare frozen-core energies with spectroscopic-term values for the sodium atom which is, of course, the united atom (UA) limit for the ammonium radical. The top block of Table III reports negative virtual orbitals energies, $-\epsilon$, for the Na^+ ion computed as described in section II. Experimental ionization energies from Moore's tables[22] (averaged over spin–orbit multiplets) are given in the second block of Table III. One observes, empirically, that the frozen-core model provides an upper bound on the true energy level of each Rydberg state of the sodium atom and that theoretical and experimental values coincide in the ionization limit. This is what one would expect if the perturbation expansion were rapidly convergent. As shown in the last block of Table III, the energy error is 1556 cm^{-1} (0.193 eV) for the 3s state and the error decreases smoothly with increasing principal or angular momentum quantum number. For ^2G states the theory agrees with experiment to within 0.1 cm^{-1}.

The Rydberg basis consists of a (20s,20p,10d,10f,10g) set of Gaussians. Tests indicate that the Rydberg orbital energies have converged to within 10 cm^{-1} of their limiting values. The core basis is a high-quality Gaussian (12s,8p) set giving E_{core} = −161.67626 hartree. This can be compared with Clementi's[23] value, $E_{SCF}(Na^+)$ = −161.67676 hartree, obtained by using a (5s,4p) Slater basis optimized for Na^+. Virtual orbital energies are reasonably insensitive to the quality of the core orbitals defining the Fock operator. For example, replacing our (12s,8p) set by a (10s,5p) core, giving E_{core} = −161.60725 hartree, shifts the calculated 3s orbital energy level by only 94 cm^{-1}. No other levels are shifted as much as 17 cm^{-1}. In other words, the virtual orbital energy shifts are at least 2 orders of magnitude smaller than the shift in the E_{core} value.

Ammonium Radical. Table IV reports Rydberg orbital properties for the ammonium radical computed under T_d symmetry with N–H bond length equal to 1.0098 Å. Our standard 51-term core and 149-term Rydberg bases were used. The table lists orbital symmetries followed by the corresponding UA designation in parentheses. Energy values (in hartrees) are computed by eq 16. The rms orbital radius (in bohrs), the angular momentum, and the Coriolis coupling constant are each computed as the appropriate integral over the occupied Rydberg orbital.

$$\langle r^2\rangle^{1/2} = \langle\phi_k|\hat{r}^2|\phi_k\rangle^{1/2} \tag{19}$$

$$\langle L^2\rangle = \hbar^{-2}\langle\phi_k|\hat{L}^2|\phi_k\rangle \tag{20}$$

$$\zeta = \hbar^{-1}\langle\phi_k|\hat{L}_z|\phi_k\rangle \tag{21}$$

This last expectation value (eq 21) is sensitive to choice of phase. For triply degenerate representations we define ϕ_k to be the complex orbital which transforms under T_d like spherical harmonics $Y_{1,1}$ and $Y_{2,-1}$. This convention[12] leads to

$$\zeta = \left\langle \phi_x \middle| x\frac{\partial}{\partial y} - y\frac{\partial}{\partial x}\middle| \phi_y \right\rangle \tag{22}$$

where $\{\phi_x, \phi_y, \phi_z\}$ are the real MO's which transform like $\{x, y, z\}$. The orbital angular momentum properties are obviously very close to their UA values. In the $^2T_2(3p)$ state, for example, the $\langle L^2\rangle$ and ζ values are about what one would expect of an almost pure atomic p orbital with 0.3% d character. The quantum defect, δn_k, is obtained from the orbital energy according to

$$\epsilon_k = -\tfrac{1}{2}(n_k - \delta n_k)^{-2} \tag{23}$$

where n_k is the principal quantum number. Column six in Table IV reports the amount (in angstroms) by which the equilibrium N–H bond length is increased for each Rydberg state when the radical is constrained to have T_d symmetry. This was computed by repeating the calculation for four different N–H bond lengths, fitting E_{core} and ϵ_k by polynomials, and determining the minimum of E_k^{FC} defined by eq 10. Thus, the predicted equilibrium bond length is

$$R_k = 1.0098\ \text{Å} + \delta R_k \tag{24}$$

In the absence of electron correlation corrections we suspect that the predicted shifts are more meaningful than the absolute bond lengths themselves.

An f-type shell on nitrogen contains an a_1, t_1, and two t_2 components under T_d symmetry and so contributes to all core orbitals and to most low-lying Rydberg MO's. A final test was carried out to determine the effect of adding such functions to our core and Rydberg bases. It also serves to check our method of computing virtual orbitals. A conventional (single basis) Roothaan SCF calculation was performed by using the 121-term basis described above. It contains two f shells optimized for the core and three more in the 3s and 4s region. If the ammonium radical is inscribed in a cube, then an f_{xyx} function has a_1 symmetry and can shift probability density from the four vacant cube corners to the other four corners where the protons are located. Results of the test calculation are compared in Table V with results using our standard bases. The E_{core} value has been lowered by almost 1 mhartree to give a record-breaking value E_{SCF} = −56.566521 hartree for the ammonium ion, but the first Rydberg orbital energy, ϵ_{3s}, has been lowered only 8.6 μhartree (2 cm^{-1}). Other orbital properties are also little affected by f-orbital contributions. For example, the increase in angular momentum expectation value

(22) C. E. Moore, "Atomic Energy Levels", Vol. I, National Bureau of Standards, Washington, DC, 1949, NBS Circular No. 467.
(23) E. Clementi, "Tables of Atomic Functions", supplement to *J. Res. Dev.*, **9**, 2 (1965), see Table 17-1.

Table IV. Rydberg Orbital Properties for the Ammonium Radical Computed Using Standard Bases[a]

orbital	ϵ_k	$\langle r^2\rangle^{1/2}$	$\langle L^2\rangle$	ξ	δR_k	$\delta n_k(NH_4)$	δn_k(Na)
a_1(3s)	−0.146 579 8	5.612	0.0751	0.0	0.006 20	1.1531	1.3415
t_2(3p)	−0.093 427 0	7.784	2.0133	0.9940	−0.001 50	0.6866	0.8624
a_1(4s)	−0.061 129 8	13.13	0.0307	0.0	0.001 69	1.1400	1.3293
t_2(3d)	−0.059 796 2	9.869	5.9707	−0.9764	0.002 61	0.1083	0.0030
e(3d)	−0.056 349 7	10.95	6.0003	0.0	−0.000 13	0.0212	0.0030
t_2(4p)	−0.044 893 7	16.81	2.0338	0.9834	−0.000 57	0.6627	0.8477
t_2(4d)	−0.033 766 7	20.26	5.9706	−0.9794	0.001 44	0.1520	0.0041
a_1(5s)	−0.033 497 9	23.78	0.0147	0.0	0.000 64	1.1365	1.3258
e(4d)	−0.031 728 1	22.01	6.0002	0.0	−0.000 05	0.0303	0.0041

[a] See eq 19-23. Geometry is T_d with R_{NH} = 1.0098 Å. Orbital energy in units of hartrees; rms radius in bohrs; δR_k in angstroms.

Table V. Results of Test Calculation Using f-Type Functions in the Core and Rydberg Basis and Comparison with Results Using Standard Bases[a]

core basis	[20,1,1,5/3,2] n_c = 121	[6,1,1/3,2] n_c = 51
Rydberg basis	[20,1,1,5/3,2] n = 121	[20,13,11/3,1] n = 149
E_{core}	−56.566521	−56.565547
ϵ_{1s}	−15.936445	−15.936618
ϵ_{2s}	−1.556382	−1.556210
ϵ_{2p}	−1.007730	−1.007805
ϵ_{3s}	−0.146588	−0.146580
ϵ_{4s}	−0.061126	−0.061130
ϵ_{5s}	−0.033504	−0.033498
$\langle r^2\rangle_{3s}^{1/2}$	5.6129	5.6122
$\langle r^2\rangle_{4s}^{1/2}$	13.1274	13.1267
$\langle r^2\rangle_{5s}^{1/2}$	23.7706	23.7831
$\langle L^2\rangle_{3s}$	0.0777	0.0751
$\langle L^2\rangle_{4s}$	0.0329	0.0307
$\langle L^2\rangle_{5s}$	0.0370	0.0147

[a] Geometry is T_d with R_{NH} = 1.0098 Å.

implies that the f functions contribute only 2×10^{-4} fractional $l = 3$ character to the 3s and 4s orbitals. This contribution rises to 2 parts per thousand for the 5s MO, even though the range of a_i values does not quite extend into the 5s region. This probably reflects the smaller gap between 4f and 5s energies. The test calculation actually gives ϵ_{4s} to be 4.2 μhartree above that obtained with the standard bases. This is probably due to omission of the diffuse d functions. We conclude that lack of f-type polarization functions in our standard bases is of little importance.

Table VI lists all transitions terminating in one of the five lowest Rydberg levels. Two different calculated frequencies are reported for each transition. The frozen-core-model prediction is the difference of orbital energies from Table IV converted to wavenumber units. Just beneath that is given a "corrected value" obtained by assuming that the correction to the frozen-core energy is independent of N–H bond length, i.e., is that given at the bottom of Table III. For example, we show the arithmetic for the $^2T_2$(3d) → $^2A_1$(3s) transition.

$$\bar{\nu} = 219475(0.1465798 - 0.0597962) + 1556 - 60 = 20543\ \text{cm}^{-1} \quad (25)$$

The third entry for each transition is the dipole transition moment computed by using our frozen-core orbitals.

Vibronic Effects. Tables VII and VIII describe the variation of E_{core} and ϵ_k, respectively, accompanying small displacements from the reference geometry. For very small vibrational distortions E_k^{FC} varies linearly due to changes in the orbital energy. This is responsible for the small shifts in R_{NH} discussed above, the splitting of degenerate electronic states, and associated static Jahn–Teller distortion. Both E_{core} and ϵ_k give rise to quadratic terms in the E_k^{FC} potential energy function, but the dominant contribution to harmonic force constants is always the E_{core} term. First we discuss E_{core} and then return to orbital energy effects.

Yamaguchi and Schaefer[24] have carried out a thorough study of harmonic force constants for NH_4^+, methane, and related small molecules and have discussed basis set effects and correlation corrections. To establish a link between our work and theirs we calculated SCF harmonic force constants for NH_4^+ using our standard core basis. We find the optimum N–H bond length to be 1.0097 Å (just 0.0001 Å less than our chosen reference geometry). This is 0.001 Å less than the R_{NH} value obtained by using their extended basis set (EBS). Our E_{core} value, −56.56555 hartree, is a slight improvement over their EBS-SCF energy of −56.56453 hartree. As reported in Table VII, the two studies give very nearly the same SCF harmonic force constants. Since experimental gas-phase data are not available for NH_4^+, we thought

Table VI. Frozen-Core Frequencies and Transition Moments for the Ammonium Radical[a]

	lower state				
upper state	$1A_1$(3s)	$1T_2$(3p)	$2A_1$(4s)	$2T_2$(3d)	1E(3d)
2E(4d)	25207	13541	6453	6160	5404
	26735	13980	6749	6192	5435
	0	0.498	0	0.246	0
$3A_1$(5s)	24819	13153	6065	5772	5015
	26254	13499	6268	5711	4955
	0	0.658	0	0.122	0
$4T_2$(4d)	24760	13094	6006	5713	4956
	26287	13532	6301	5744	4988
	0.037	0.022	0.297	0.389	0.105
$3T_2$(4p)	22318	10652	3563	3271	2514
	23737	10982	3751	3194	2438
	0.278	0.242	6.871	2.665	3.973
1E(3d)	19803	8138	1049	756	
	21300	8544	1314	756	
	0	3.942	0	0.494	
$2T_2$(3d)	19047	7381	293		
	20543	7788	558		
	0.091	3.374	0.620		
$2A_1$(4s)	18754	7088			
	19986	7231			
	0	3.001			
$1T_2$(3p)	11666				
	12755				
	3.199				

[a] For each entry the top number is the frequency in cm^{-1} from Table IV. The next entry is a corrected frequency computed as in eq 25. The third entry is the transition moment in units of bohrs.

Table VII. Comparison of Calculated Bond Length and Force Constants for the Ammonium Ion with Relevant Literature Values

	NH_4^+		CH_4	
	this work	EBS SCF[b]	EBS SCF[b]	expt
F_{11}[a]	7.604	7.556	5.898	5.842
F_{22}	0.684	0.679	0.553	0.486
F_{33}	7.420	7.400	5.698	5.383
F_{44}	0.655	0.649	0.527	0.458
F_{34}	0.174	0.166	0.205	0.206
R^c	1.0097	1.0107	1.0823	1.0858
E_{SCF}	−56.56555	−56.56453	−40.21383	

[a] Harmonic force constants in units of mdyn/Å. [b] Extended basis set SCF results from ref 24. [c] Equilibrium bond length in angstroms.

(24) Y. Yamaguchi and H. F. Schaefer, *J. Chem. Phys.*, **73**, 2310 (1980).

Table VIII. First and Second Derivatives of Orbital Energies with Respect to Vibrational Distortion along Standard Symmetry Coordinates[a]

orbital symmetry				T_d, A_1 stretch $\equiv S_1$		C_{3v}, T_2 stretch $\equiv S_3$		C_{3v}, T_2 bend $\equiv S_4$		D_{2d}, E bend $\equiv S_2$	
UA	T_d	C_{3v}	D_{2d}	$\partial\epsilon/\partial S_1$	$\partial^2\epsilon/\partial S_1^2$	$\partial\epsilon/\partial S_3$	$\partial^2\epsilon/\partial S_3^2$	$\partial\epsilon/\partial S_4$	$\partial^2\epsilon/\partial S_4^2$	$\partial\epsilon/\partial S_2$	$\partial^2\epsilon/\partial S_2^2$
3s	a_1	a_1	a_1	−21000	−86 000	0	−106 000	0	−14900	0	−5830
3p	t_2	a_1	b_2	4780	−15 300	−5260	−17 200	−5280	−2930	8060	−3450
		e	e	4780	−15 300	2630	−13 700	2640	−236	−4030	127
4s	a_1	a_1	a_1	−6240	−23 500	0	−301 000	0	−17900	0	−4410
3d	t_2	a_1	b_2	−9390	−23 700	−16600	−179 000	416	6860	−9000	−14400
		e	e	−9390	−23 700	8300	−13 600	−208	−3870	4500	−1370
3d	e	e	a_1	25	991	0	6 140	0	3520	2360	406
			b_1	25	991	0	6 140	0	3520	−2360	−51
4p	t_2	a_1	b_2	1560	−5 440	−1430	−25 200	−1570	−875	2400	−913
		e	e	1560	−5 440	717	−5 230	783	−194	−1200	0
4d	t_2	a_1	b_2	−5410	−11 800	−9100	−324 000	718	−20700	−4940	−16100
		e	e	−5410	−11 800	4550	−5 760	−359	−1730	2470	−659
5s	a_1	a_1	a_1	−2650	−9 570	0	170 000	0	15000	0	5500
4d	e	e	a_1	−262	25 300	0	2 530	0	1330	1010	608
			b_1	−262	25 300	0	2 530	0	1330	−1010	0
E_{core}				427	1 744 000	0	1 702 000	0	150200	0	156900

[a] Derivatives computed at reference geometry (T_d symmetry with R_{NH} = 1.0098 Å) by using standard basis sets. First and second derivatives in units of μhartree/Å and μhartree/Å², respectively. 1 hartree = 4.3598 mdyn Å.

it would be useful to include in Table VI a comparison of experimental and theoretical harmonic force constants for the isoelectric methane molecule. For references and further discussion the reader is referred to the paper by Yamagouchi and Schaefer.[24]

The symmetry coordinates for vibration of a tetrahedral molecule may be expressed in terms of internal displacement coordinates as follows:

$$S_1 = \tfrac{1}{2}[\Delta R_1 + \Delta R_2 + \Delta R_3 + \Delta R_4] \quad (26)$$

$$S_2 = R_0 12^{-1/2}[2\Delta\theta_{12} + 2\Delta\theta_{34} - \Delta\theta_{13} - \Delta\theta_{24} - \Delta\theta_{14} - \Delta\theta_{23}] \quad (27)$$

$$S_3 = 12^{-1/2}[3\Delta R_1 - \Delta R_2 - \Delta R_3 - \Delta R_4] \quad (28)$$

$$S_4 = R_0 6^{-1/2}[\Delta\theta_{12} - \Delta\theta_{34} + \Delta\theta_{13} - \Delta\theta_{24} + \Delta\theta_{14} - \Delta\theta_{23}] \quad (29)$$

where R_0 is the reference bond length, R_0 = 1.0098 Å. The S_1, S_2, S_3, and S_4 coordinates define the a_1-type symmetric stretching, the e-type bending, the t_2-type asymmetric stretching, and the t_2-type bending displacements, respectively. Our S_1 and S_2 are identical with the standard coordinates of Easterfield and Linnet,[25] and our S_3 and S_4 are obtained by a unitary transformation of their coordinates for the triply degenerate modes.

$$S_3 = 3^{-1/2}(S_{3a} + S_{3b} + S_{3c}) \quad (30)$$

$$S_4 = R_0 3^{-1/2}(S_{4a} + S_{4b} + S_{4c}) \quad (31)$$

Distortion along S_2 lowers the symmetry from T_d to D_{2d}, and distortion along S_3 or S_4 to C_{3v}.

The core and orbital energy components of the frozen-core energy are, of course, functions of the symmetry coordinates

$$E_k^{FC}(\mathbf{S}) = E_{core}(\mathbf{S}) + \epsilon_k(\mathbf{S}) \quad (32)$$

and may be expanded in a Taylor series about the reference geometry. Table VIII reports the appropriate linear and quadratic terms. The E_{core} values given in the last time of the table lead immediately to the NH_4^+ force constants reported in Table VII. Similarly, one obtains force constants for the ammonium radical in its various Rydberg states by adding the appropriate orbital contribution, $\partial^2\epsilon/\partial S_m^2$, to the E_{core} value listed at the bottom of the same column of the table. For example, in this way one computes harmonic force constant F_{33} = 6.108 mdyn/Å for the $2^2A_1(4s)$ state. This value can be compared with F_{33} = 7.420 mdyn/Å for the ion. This is one of the largest calculated deviations from ion force constants and is in line witth other pathological behavior of the $2^2A_1(4s)$ state to be discussed below.

The small shifts in N–H bond lengths described by eq 24 and reported in Table IV may be computed from information in Table VIII as follows:

$$\delta R_k = \tfrac{1}{2}S_1^{eq} = -\tfrac{1}{2}\left[\frac{\partial(E_{core} + \epsilon_k)}{\partial S_1}\right]\left[\frac{\partial^2(E_{core} + \epsilon_k)}{\partial S_1^2}\right]^{-1} \quad (33)$$

The corresponding shift in the frozen-core energy is

$$E_k^{FC}(S_1^{eq}) = E_k^{FC}(0) + 2\delta R_k[\partial(E_{core} + \epsilon_k)/\partial S_1] \quad (34)$$

Thus, relaxing the N–H bond length lowers E_{3s}^{FC} by only 128 μhartree (28 cm^{-1}), and the effect is smaller yet for other Rydberg states.

Similarly, one can compute geometry changes and energy shifts for symmetry-breaking distortions in degenerate Rydberg states, i.e., Jahn–Teller effects. For example, a triply degenerate bend lifts the degeneracy of the $1^2T_2(3p)$ state. The A_1 component (under C_{3v} symmetry) has minimum energy when S_4 = 0.0359 Å. This corresponds to a 5° change in HNH bond angles and a Jahn–Teller energy shift

$$\Delta E_{JT} = \tfrac{1}{2}\left[\frac{\partial\epsilon_k}{\partial S_m}\right]^2\left[\frac{\partial^2(E_{core} + \epsilon_k)}{\partial S_m^2}\right]^{-1} \quad (35)$$

of 95 μhartree (21 cm^{-1}). No ΔE_{JT} values computed by using eq 35 and the data in Table VIII turn out to be as great as 65 cm^{-1}.

The most important vibronic effects are likely to be associated with mixing of nearly degenerate Rydberg orbitals during a vibrational distortion. For example, one notes from Table IV that the $2^2T_2(3d)$ state lies only 1334 μhartree (293 cm^{-1}) above $2^2A_1(4s)$. According to Table VIII this T_2 level splits into A and E components under an asymmetric stretching distortion, and the A component descends steeply toward the lower $2^2A_1(4s)$ state. Figure 1 describes the relevant orbital energies in the vicinity of the avoided crossing. The horizontal scale measures displacement of the unique hydrogen atom, ΔR_1. From eq 28 one notes that this is proportional to the amplitude of the symmetry coordinate S_3.

$$\Delta R_1 = (3/4)^{1/2}S_3 \quad (36)$$

$$\Delta R_2 = \Delta R_3 = \Delta R_4 = -\tfrac{1}{3}\Delta R_1 \quad (37)$$

Orbital energies computed for ΔR_1 = −0.9–0.09 Å are shown in Figure 1. The solid curves in the figure have been fitted to these

(25) J. R. Easterfield and J. W. Linnett, *J. Chem. Soc., Faraday Trans. 2*, **70**, 317 (1974).

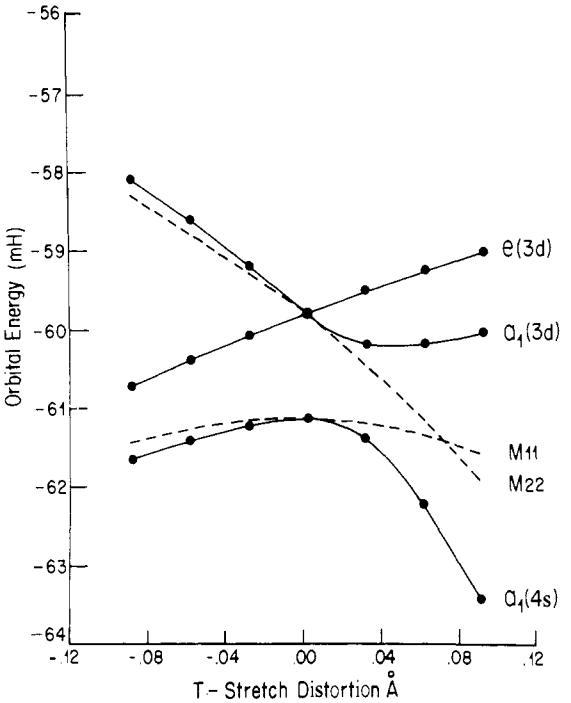

Figure 1. Variation of the $a_1(4s)$ and $t_2(3d)$ orbital energies as a function of asymmetric stretching distortion. The T_d symmetry is reduced to C_{3v} thereby splitting the degenerate t_2 level into its a(3d) and e(3d) components. The a(3d) component mixes with the lower a(4s) level. Dashed curves are energies of hypothetical unmixed orbitals. An avoided crossing occurs when the unique N–H bond is elongated 0.072 Å. Dots represent orbital energies computed directly from eq 16. Solid curves are the fitted orbital energies computed for a(4s) and a(3d) by using eq 38. Energy values are given in millihartree units. Horizontal scale measures internal coordinate ΔR_1 in units of angstroms.

points assuming that the interaction of the a(4s) and a(3d) orbitals can be described by a 2-by-2 mixing matrix.

$$\begin{pmatrix} M_{11} & M_{12} \\ M_{21} & M_{22} \end{pmatrix} \begin{pmatrix} \cos\alpha & \sin\alpha \\ -\sin\alpha & \cos\alpha \end{pmatrix} = \begin{pmatrix} \cos\alpha & \sin\alpha \\ -\sin\alpha & \cos\alpha \end{pmatrix} \begin{pmatrix} \epsilon_{4s} & 0 \\ 0 & \epsilon_{3d} \end{pmatrix} \quad (38)$$

By definition $\alpha(S_3)$ measures the orbital mixing due to this symmetry-breaking distortion and is zero for T_d symmetry. The diagonal elements $M_{11}(S_3)$ and $M_{22}(S_3)$ are the energies of the hypothetical unmixed a(4s) and a(3d) orbitals, respectively. The off-diagonal element, $M_{12} = M_{21}$, is the interaction energy which is zero, by definition, when $S_3 = 0$. We represented the e-type orbital energy component and each of the M_{ij} elements by low-order polynomials in S_3. The 20 data points in Figure 1 were fitted with nine parameters (three of which were determined immediately from the known orbital energies and their first derivatives at $S_3 = 0$). The dashed curves in Figure 1 describe the diagonal matrix elements. Note that they coincide when $\Delta R_1 = 0.072$ Å, at which point the interaction energy is computed to be $M_{12} = 275$ cm^{-1}. Note further that the amount of mixing varies from $\alpha = 0$ (none) to $\alpha = \pi/4$ (complete) over the range of a typical vibrational amplitude.

Although the mixing parameter $\alpha(S_3)$ in eq 38 has been determined by fitting energies, it has significance for other properties as well. Let us assume, as a rough approximation, that the expectation value of $\hat{L}^2$ is zero for the hypothetical unmixed a(4s) orbital and $6\hbar^2$ for the unmixed a(3d) orbital. Then we predict that the actual (mixed) a(4s) and a(3d) orbitals should have the following expectation values:

$$\hbar^{-2}\langle L^2\rangle_{4s} \approx 6 \sin^2 \alpha \quad (39)$$

$$\hbar^{2}\langle L^2\rangle_{3d} \approx 6 \cos^2 \alpha \quad (40)$$

It can be seen from Figure 2 that expectation values predicted by the frozen-core model are in qualitative agreement with this simple model.

Table IX. Dipole Transition Moments for Three Rydberg Transitions of the Ammonium Radical Distorted along the Asymmetric Stretching Coordinate, S_3

	transition moments, bohr		
ΔR_1 [a]	A(4s) → A(3s)	A(3p) → A(3s)	A(3d) → A(3s)
−0.09	−0.034	3.100	0.011
−0.06	−0.035	3.134	0.033
−0.03	−0.027	3.167	0.059
0	0.0	3.199	0.091
0.03	0.076	3.229	0.102
0.06	0.157	3.253	0.081
0.09	0.237	3.271	0.061

[a] Internal coordinate, in angstroms, defined in eq 36 and 37.

The transition moments reported in Table VI are computed for a vertical transition at the reference geometry. To treat vibronic intensities requires knowledge of these moments as a function of vibrational distortion coordinates. We do not attempt a complete analysis but present in Table IX just a sample of the available information. For each of the states discussed in Figures 1 and 2 we report the dipole transition moment for a vertical transition to the ground-state surface. Dipole selection rules for tetrahedral molecules forbid electronic transitions between two A states, but these become vibronically allowed when combined with a T_2-type vibrational transition. For example, $2^2A_1(4s)$ in its ground vibrational state is dipole coupled to $1^2A_1(3s)$ in its first excited ν_3 or ν_4 vibrational mode. Table IX reports the relevant transition moment as a function of the asymmetric stretching coordinate. The function shows marked deviation from linearity implying vibronic transitions with $\Delta v = 1, 2, \ldots$. However, all these transitions are predicted to be 2 orders of magnitude weaker than the strong $1^2T_2(3p) \rightarrow 1^2A_1(3s)$ emission with $\Delta v = 0$. The vibronic transition is predicted by this calculation to be comparable in intensity to the allowed but weak $2^2T_2(3d) \rightarrow 1^2A_1(3s)$ transition.

IV. Discussion

With modern methods, it is possible to far surpass the accuracy of the one-center, ab initio calculations of Strehl et al.,[5] but it is noteworthy that the ammonium radical Rydberg levels predicted in that early study are in qualitative agreement with ours. A much more significant comparison is possible with the very recent calculations of Raynor and Herschbach (RH),[15b] who also used the frozen-core model but in a Slater-type orbital (STO) basis with floating STO-1s functions "on" the hydrogen atoms. The NH_4^+ SCF energies provide one measure of the accuracies attained in these calculations, namely, the following: $E_{core} = -55.80859$ hartree, Strehl et al.;[5] $E_{core} = -56.45886$ hartree, Raynor and Herschbach;[15b] $E_{core} = -56.56453$ hartree, Yamaguchi and Schaefer;[24] $E_{core} = -56.56555$ hartree, this work, standard basis; $E_{core} = -56.56652$ hartree, this work, best SCF. The quantum defects reported by RH converted to orbital energies give $\epsilon_{3s} = 148555$ μhartree, $\epsilon_{4s} = 58553$ μhartree, and $\epsilon_{5s} = 29820$ μhartree. These differ from ours, in Tables IV and V, by a few millihartrees. When our values are adjusted to $R_{NH} = 1.0208$ Å, the bond length used by RH, their ϵ_{3s} value lies 1492 μhartree (327 cm^{-1}) below ours. This discrepancy is 2 orders of magnitude smaller than the error in their E_{core} value, so we attribute it to their somewhat different $\hat{H}^\circ$ operator. Their ϵ_{4s} and ϵ_{5s} values lie 2720 and 3739 μhartree above our adjusted values. This is probably due to a combination of $\hat{H}^\circ$ and Rydberg basis set deficiencies. All e- and t_2-type orbital energies computed in the two studies agree to within 220 cm^{-1}. Consistent results have also been obtained by Wright.[26] Thus, three independent frozen-core-model calculations concur to within the expected precision. More serious questions remain concerning the accuracy of the model. It is certainly much more reliable for transitions involving one electron outside a closed shell than for ionization potentials of valence electrons.[27] Table III

(26) J. Wright, private communication.
(27) I. Hubac and M. Urban, *Theor. Chim. Acta*, **45**, 185 (1977).

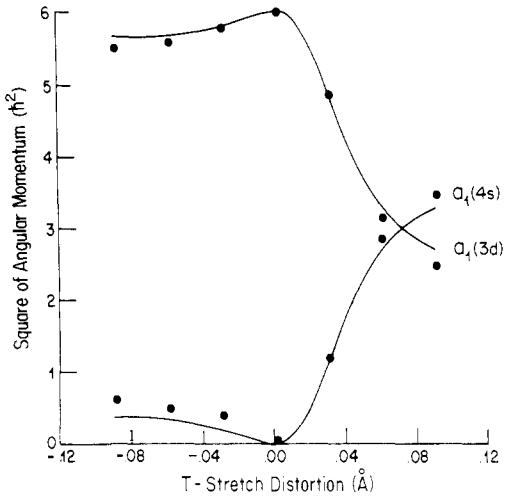

Figure 2. Expectation value of $\hat{L}^2$ for a(4s) and a(3d) levels. Dots represent values computed directly from eq 20. Solid curves are computed according to eq 39 and 40 by using α values from eq 38. Vertical scale is in units of $\hbar^2$. Horizontal scale measures internal coordinate ΔR_1 in units of angstroms.

reports the corrections that must be applied for sodium. We expect that comparable corrections (1600 cm^{-1} or less) should be applied to the computed ammonium radical energy levels, as has been done in Table VI. In this connection it is noteworthy that assigned band origins for observed Rydberg transitions in triatomic hydrogen[7-10] all agreed with frozen-core-model predictions[12] to within 1500 cm^{-1} and that the theory gave satisfactory Coriolis coupling constants and Jahn–Teller parameters. The model appears to be considerably less reliable for spectroscopic intensities. Raynor and Herschbach make this same observation and point out that improved emission coefficients are obtained by using a valence bond formalism.[15]

If one accepts the general validity of the preceding remarks, then it is difficult to reconcile our theoretical results with all of the available experimental observations on NH_4 and ND_4 radicals. Schüler, Michel, and Grün[28] and earlier spectroscopists (dating back to A. Schuster in the 19th century) have reported what appears to be a single band system with unresolved rotational structure observed in emission from ammonia in discharge tubes. The diffuse bands reported at 7666, 6497, 5672, 5639, and 5282 Å (13 040, 15 390, 17 630, 17 730, and 18 930 cm^{-1} respectively) were once attributed to NH_3 and then later to (perhaps) N_2H_4. Recent investigation by Herzberg[10] has established that these are features of the Rydberg spectrum of NH_4, and he has given them the name "Schuster bands". The corresponding spectrum of ND_4, which is sharper and more intense, exhibits broadened yet resolved rotational structure extending from 17 180 to 17 350 cm^{-1} with band origin in the vicinity of 17 240 cm^{-1}. These correspond to the emission features observed near 5672 and 5639 Å in NH_4. The other NH_4 features presumably also have their counterparts in the ND_4 spectrum, but only a cursory discussion of these can be found in the literature.[28] Herzberg has assigned the Schuster band to $^2T_2(3d) \rightarrow {}^2A_1(3s)$. The frozen-core model predicts this transition to be very weak and to occur at 19 047 cm^{-1}. The 1800-cm^{-1} discrepancy between theory and observation is disturbing because corrections to the model are expected to lower the ground state more than the excited state thereby increasing the discrepancy to more than 3000 cm^{-1}. On the other hand, there exists no reasonable alternative assignment. The $^2A_1(3s)$ and $^2T_2(3p)$ states are the only Rydberg levels with ionization energies greater than 17 000 cm^{-1} so one of these two must be the lower state for the transition. If it were $^2T_2(3p)$ then the upper state would have an unlikely high principal quantum number; furthermore, it would be expected to exhibit a spin–orbit doublet (not observed in the Schuster band). Herzberg argues that the observed PQR rotational structure corresponds to a Coriolis coupling constant near $\zeta = -1$ implying d → s character for the transition.[10] This is supported by our calculations; in particular, we calculate $\zeta = -0.9764$ for the $^2T_2(3d)$ upper state. Diffuseness of the Schuster band is attributed to the finite lifetime of the metastable $^2A_1(3s)$ ground state. This is in conflict, however, with molecular-beam results which imply that the lifetime of the ground state is about 1 μs,[11] far too long to account for the observed line widths.

A second band system, the so-called Schüler band,[10] is observed in the region 15 050–15 210 cm^{-1} in NH_4, 14 810–14 940 cm^{-1} in ND_4. The rotational structure is much better resolved and spin–orbit doubling is observed. Herzberg tentatively assigns the Schüler band to $^2E(3d) \rightarrow {}^2T_2(3p)$. This is in serious conflict with the frozen-core model which predicts this transition to occur at 8138 cm^{-1} (at 8544 cm^{-1} using the corrected value in Table VI). The doublet structure implies involvement of the $^2T_2(3P)$ so there seem to be only four likely candidates (numbers in parentheses are corrected frequencies computed by using eq 25: $^2T_2(3p) \rightarrow {}^2A_1(3s)$, 11 666 cm^{-1} (12 755 cm^{-1}); $^2E(4d) \rightarrow {}^2T_2(3p)$, 13 541 cm^{-1} (13 980 cm^{-1}); $^2A_1(5s) \rightarrow {}^2T_2(3p)$, 13 153 cm^{-1} (13 499 cm^{-1}); $^2T_2(4d) \rightarrow {}^2T_2(3p)$, 13 094 cm^{-1} (13 532 cm^{-1}). Herzberg rejects the $^2T_2(3p) \rightarrow {}^2A_1(3s)$ assignment on the basis of the narrow lines in the Schüler band. Raynor and Herschback[15b] suggest this band be assigned to $^2A_1(5s)$ or $^2A_1(6s) \rightarrow {}^2T_2(3p)$. We have no way of distinguishing these candidates and defer the Schüler assignment until paper 3 of this series.

It is interesting to consider the possibility that the Schuster band terminates in the first excited vibrational state of the asymmetric stretching mode. This is thought to have a frequency[24] of about 3379 cm^{-1} in NH_4 (probably near 2270 cm^{-1} in the ground state of the ND_4 radical). One might further hypothesize that the Schüler band terminates in the ground vibrational state of $^2A_1(3s)$. This would resolve the conflict between spectroscopic and molecular-beam lifetimes and would bring the observed frequencies in line with theory. Perhaps the Schuster band is a vibronically allowed transition discussed in connection with Table IX. This would explain the absence of the corresponding $\Delta v = 0$ transition. The rotational structure would be complicated by the vibrational as well as the electronic Coriolis coupling. A serious argument against this hypothesis is the isotope effect, i.e., the observation that the Schuster band in NH_4 is observed 440 cm^{-1} to the blue of that in NH_4. Our suggestion implies that it would be shifted about 900 cm^{-1} to the red, i.e., near 6130 Å.

V. Conclusion

With large Gaussian basis sets it is possible to solve the frozen-core model for excited states of NH_4 to high accuracy, probably to within 10 cm^{-1}. Serious conflicts arise in comparing the frozen-core-model, spectroscopic, and molecular-beam results. There is a need to extend the theory to include the following: (A) correlation energy corrections to frozen-core energies, particularly for Rydberg levels with principal quantum number $n = 3$, (B) correlation corrections to spectroscopic transition probabilities, (C) a reliable theoretical prediction of the lifetime of NH_4 and ND_4 in its metastable ground state. These topics will be the subject of future papers in this series.

Acknowledgment. Acknowledgment is made to the donors of the Petroleum Research Fund, administered by the American Chemical Society, for paartial support of this research. We thank G. Herzberg, J. Hougen, S. Raynor, and D. Herschbach for stimulating discussions and absolve them of any blame for our views concerning the assignment of the NH_4 spectrum. Computer time was supplied under a grant from the National Resource for Computation in Chemistry.

Appendix

Let **A** be the rectangular matrix obtained by applying a Schmidt process to **B** defined in eq 13. Let

$$\mathbf{P} \equiv \mathbf{I} - \mathbf{A}\mathbf{A}^{\dagger} \tag{A1}$$

so that **P** is a projection operator that preserves the vector space

(28) H. Schüler, A. Michel, and A. E. Grün, *Z. Naturforsch. A*, **10**, 1 (1955).

orthogonal to columns of **B**. In particular, **P** satisfies the equation

$$\mathbf{PB} = \mathbf{O} \tag{A2}$$

Let **U** be a unitary matrix which diagonalizes the Hermitian matrix **PSP** where **S** is defined in eq 12.

$$(\mathbf{PSP})\mathbf{U} = \mathbf{U}\lambda \tag{A3}$$

Let **Q** be a rectangular matrix with elements

$$Q_{ij} = U_{ij}\lambda_{jj}^{-1/2} \tag{A4}$$

where columns of **Q** are simply omitted if the corresponding eigenvalue λ_{jj} is below some tolerance, e.g., $\lambda_{jj} > 10^{-6}$. It follows that **Q** satisfies eq 14 and 15.

Registry No. NH_4, 14798-03-9; ND_4, 83682-14-8; Na, 7440-23-5.

Nuclear Magnetic Shielding in Cyclopropane and Cyclopropenyl Cation

P. Lazzeretti,* E. Rossi, and R. Zanasi

Contribution from the Istituto di Chimica Organica e Centro di Calcolo Elettronico dell'Università di Modena, I-41100 Modena, Italy. *Received March 8, 1982*

Abstract: The magnetic shielding tensors of the proton and carbon nuclei have been rationalized by coupled Hartree–Fock theoretical studies. Orbital contributions are systematically analyzed and electron current density maps are shown, indicating the typical paramagnetic axial vortex of cyclic molecules. Satisfactory agreement with experimental carbon chemical shift data has been found for cyclopropane. The results show that any ring current hypothesis in either of these molecules is misleading.

Introduction

In previous papers we attempted to rationalize the characteristic magnetic properties of cyclopropenyl cation[1] and benzene[2,3] by visualizing the stationary flow of electron density induced by a uniform magnetic field.

The main features emerging from these studies[1-3] are the following. (i) As a mere consequence of symmetry, all planar cyclic molecules are endowed with a paramagnetic axial vortex[4,5] due to σ electrons flowing around the highest symmetry axis. (ii) In aromatic rings the intensity of such a vortex is high enough to overcome the diamagnetic "ring current" of π electrons. (iii) Quasi-toroidal vortices are found near each of the skeletal carbon atoms, perpendicular to the molecular plane. (iv) In benzene[2,3] the electron circulation in the neighborhood of each carbon deviates significantly from the shape of a perfect geometrical torus in such a way that the perpendicular component of carbon magnetic shielding is unusually upfield ($\sigma_{33}(C) \approx 190$ ppm in benzene[2].

There is recent experimental evidence[6] that nonaromatic rings, such as cyclopropane, are also characterized by an anomalous high-field value of $\sigma_{33}(C)$. This paper sets out to explain this behavior in cyclopropenyl cation and cyclopropane through an analysis of theoretical nuclear shielding and electron density maps.

Results and Discussion

The theoretical approach and the computational scheme employed in this study have been previously outlined in detail.[1-3] The Gaussian basis sets used in the calculation for the ion are the same as in a previous study,[1] e.g., (11s7p2d/5s1p) contracted to [6s5p$_x$5p$_y$7p$_z$1d/3s1p]. The same primitive basis is used for cyclopropane, contracted to [6s5p1d/3s1p] (117 contracted functions). The geometry assumed in the calculation is that adopted in ref 1. For cyclopropane we retained the geometry of ref 10, as specified in Table I here.

Since the polarization functions have exponents optimized for the magnetic properties, our self-consistent field (SCF) energy for C_3H_6, which is -117.089055 hartree, is ≈5 mhartree higher than the best previous value[7], -117.0945. However, a number of results indicate the near-Hartree–Fock (HF) character of our wave function for cyclopropane. In particular, for the Arrighini–Maestro–Moccia (AMM) tensors,[8] denoting the components parallel to the C_3 axis by ∥, we found $(P_{\parallel},P_{\parallel}) = 22.893$; $(P_{\perp},P_{\perp}) = 22.601$, i.e., ≈95% of the exact value of 24. Adopting a slightly different definition with respect to our previous paper[9] for the magnetic perturbation, e.g., explicitly including the imaginary unit i, we introduce

$$h^{H_\alpha} = -(i/2c)\epsilon_{\alpha\beta\gamma}r_\beta\nabla_\gamma \tag{1}$$

$$h^{(dxH)_\alpha} = -(i/2c)\nabla_\gamma \tag{2}$$

$$h^{\mu_\alpha}(N) = -(i/c)|\mathbf{r} - \mathbf{R}_N|^{-3}\epsilon_{\alpha\beta\gamma}(r - R_N)_\beta\nabla_\gamma \tag{3}$$

possessing representations on the LCAO basis

$$\mathrm{H}^{H_\alpha} \tag{1'}$$

$$\mathrm{H}^{(dxH)_\alpha} \tag{2'}$$

$$\mathrm{H}^{\mu_\alpha}(N) \equiv \mathrm{H}^{\mu_\alpha} \tag{3'}$$

The (P,P) tensor is defined as

$$(P_\alpha,P_\beta) = -8c^2\mathrm{Tr}\mathrm{H}^{(dxH)_\alpha}\mathbf{R}^{(dxH)_\beta} \tag{4}$$

and satisfies the sum rule (5), valid for exact HF functions

$$(P_\alpha,P_\beta) = N\delta_{\alpha\beta} \tag{5}$$

Owing to the form of the exact coupled Hartree–Fock (CHF) perturbed orbitals, it can be easily shown that (5) is a direct

(1) Lazzeretti, P.; Zanasi, R. *Chem. Phys. Lett.* **1981**, *80*, 533.
(2) Lazzeretti, P.; Zanasi, R. *J. Chem. Phys.* **1981**, *75*, 5019.
(3) Lazzeretti, P.; Zanasi, R. *Nuovo Cimento D* **1982**, *1*, 70; *J. Chem. Phys.* **1982**, *77*, 3129.
(4) Riess, J. *Ann. Phys.* **1970**, *57*, 301; **1971**, *67*, 347; *Phys. Rev. D* **1970**, *2*, 647; *Phys. Rev. B* **1976**, *13*, 3862.
(5) Hirschfelder, J. O. *J. Chem. Phys.* **1977**, *67*, 5477; Heller, D. F.; Hirschfelder, J. O. *Ibid.* **1977**, *66*, 1929; Corcoran, C. T.; Hirschfelder, J. O. *Ibid.* **1980**, *72*, 1524.
(6) Zilm, K. W.; Conlin, R. T.; Grant, D. M.; Michl, J. *J. Am. Chem. Soc.* **1980**, *102*, 6672; Zilm, K. W.; Beeler, A. J.; Grant, D. M.; Michl, J.; Teh-Chang Chou; Allred, E. L. *Ibid.* **1981**, *103*, 2119.
(7) Amos, R. D.; Williams, J. H. *Chem. Phys. Lett.* **1981**, *84*, 104.
(8) Arrighini, G. P.; Maestro, M.; Moccia, R. *J. Chem. Phys.* **1968**, *49*, 882.
(9) Lazzeretti, P.; Zanasi, R. J. *Chem. Phys.* **1978**, *68*, 832; **1977**, *67*, 382.
(10) Bastiansen, O.; Fritsch, F. N.; Hedberg, K. *Acta Crystallogr.* **1964**, *17*, 538.

0002-7863/83/1505-0012$01.50/0